

Received November 27, 2018, accepted December 13, 2018, date of publication January 11, 2019, date of current version February 4, 2019.

Digital Object Identifier 10.1109/ACCESS.2019.2892228

# Novel Channel Quality Indicator Prediction Scheme for Adaptive Modulation and Coding in High Mobility Environments

RONG ZENG<sup>1</sup>, TIANJING LIU<sup>1</sup>, XUTAO YU<sup>2</sup>, AND ZAICHEN ZHANG<sup>2</sup>, (Senior Member, IEEE)

<sup>1</sup>School of Communications Engineering, Hangzhou Dianzi University, Hangzhou 310018, China

<sup>2</sup>School of Information Science and Engineering, Southeast University, Nanjing 210096, China

Corresponding author: Rong Zeng (zengrong@hdu.edu.cn)

This work was supported by the National Natural Science Foundation of China under Grant 61871111 and Grant 61571105.

**ABSTRACT** In this paper, a novel channel quality indicator (CQI) prediction scheme for adaptive modulation and coding in high-speed mobility environments is proposed, where the wavenumber spectrum segmentation filters' bank is utilized to improve the estimation accuracy of channel prediction algorithm by enhancing the correlation of wireless channels in each orthogonal subspace. In the proposed method, the channel estimation, channel prediction, and signal-to-noise-rate (SNR) prediction are processed on the orthogonal subspace level, which can significantly decrease the mismatch level of the feedback CQI under the fast time-varying channels. Based on the predicted SNR after subspace signal combination, the effective SNR is obtained and is utilized to calculate the feedback CQI parameter. The autocorrelation function and spatial fading rate are analyzed with different feedback delays, which show that our proposed scheme provides stronger correlation of channels with the order of wavenumber spectrum segmentation filters' bank increasing. The simulation results show that the proposed scheme can achieve better throughput performance even with larger feedback delay in high-speed mobility environments.

**INDEX TERMS** Time-varying channels, wavenumber spectrum segmentation filters bank, adaptive modulation, mobile communication.

## I. INTRODUCTION

Wireless broadband access technology in high speed mobility is taken as one of the key features in 5G system, whose speed can reach up to 500 km/h [1]. However, the fast time-varying channel strictly limits the throughput performance of 5G system. AMC is an effective technology to match the varying channel condition dynamically, which has been widely adopted in broadband wireless communication systems to provide high data rate wireless services. The concept of AMC originated from adaptive transmission system in the late 1960s [2]–[4]. Currently, AMC technique research mainly focuses on the mode selection method [5]–[7], channel coding improvement [8], accurate CSI acquisition and AMC implementation [9]. Based on information theoretical results, the constellation and channel coding rate selection problem in AMC for MIMO systems was studied [5].

However, in high mobility scenes, the performance of AMC system is significantly deteriorated resulting from rapidly time-varying channels. Reliable channel prediction to forecast the channel variation is necessary. The channel

prediction algorithm usually adopt the autoregressive (AR) predictive modeling [10], [11] or deterministic parameters based modeling [12]. Assuming a wide sense stationary channel, AR modeling based channel prediction calculates the channel state through its previous states and the temporal channel correlation has to be evaluated through training [10], [11]. However, in the non-stationary and fast-varying environment, the temporal correlation of channel coefficients are difficult to be obtained. The deterministic parameters based modeling is applied under the assumption of quasi-static channel, which requires the number of propagation paths to be invariant.

In this paper, a novel CQI prediction scheme based on wavenumber spectrum segmentation filters bank for AMC in high mobility environments is proposed. The similar implementation of wavenumber spectrum segmentation filters in high mobility condition for synchronization and symbol detection is shown in our previous published article [13]–[15]. Similarly, Svantesson and Swindlehurst [16] proposed an AR-BF channel predict

scheme which projects the receive signal onto several angular regions, thus resolving the signal with large number of complex sinusoids into several components with a smaller number of rays. Different from [16], in our proposed scheme, sub-space wavenumber spectrum is shifted to enhance the temporal domain correlation of the channel parameters, which lower the channel time-varying level of each orthogonal subspace. This makes that we can adopt lower complexity channel prediction algorithm such as linear extrapolation in our proposed scheme, rather than the AR prediction in [16]. Moreover, this enhanced correlation suppresses the CQI mapping mismatch further. The predicted SNRs on all orthogonal subspaces are combined and the effective SNRs is calculated through the effective SNR mapping (ESM) algorithm with the equivalent SNRs.

The remainder of this paper is organized as follow. In Section II, the motivation and system model are presented firstly. In Section III, a novel wavenumber spectrum segmentation filters bank based CQI prediction scheme in high mobility environment is proposed. Moreover, theoretical analysis of autocorrelation, spatial fading rate variance and simulation results are presented in Section IV. Finally, Section V concludes this paper.

**II. MOTIVATIONS AND SYSTEM MODEL**

In this section, the motivation of this paper to improve the performance of the CQI prediction for AMC scheme in high mobility environments is described and the system model is also described in detail. This paper focuses on the problem of CQI mismatch for time-varying channel aroused by high mobility. In addition, multiple antennas system is adopted as system model to evaluate the performance.

**A. MOTIVATIONS**

The AMC scheme procedure in receiver is shown as Fig. 1. The channel parameter is estimated by received signal. And the estimated channel condition parameter is feedback to the transmitter side. The feedback CQI value may not reflect the actual channel condition when the next transmitted signal is scheduled. The mismatch arises from the following aspects:

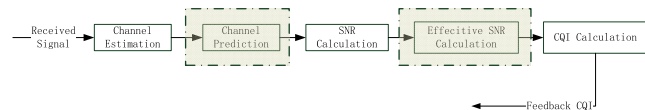


**FIGURE 1. AMC scheme procedure in receiver.**

1) The time delay including the CQI propagation delay, feedback channel schedule delay and traffic channel schedule delay. These cause the channel condition difference between CQI measurement time and CQI utilizing time.

2) The time-varying channel parameter. This is aroused mainly from high mobility, which leads to the channel condition difference between received measurement instant and traffic schedule instant;

3) CQI mapping accuracy. More intense channel changing level makes frame level CQI evaluation more inaccurate.

To suppress the effect of the CQI feedback delay and timing-varying channel, channel prediction is adopted in the receiver to predict the channel condition when the next scheduled signal is actually transmitted. Most of the channel prediction algorithms are based on certain prediction model. The higher the matching degree between prediction model and the signal to be predicted, the better the performance. In practical application, the same CQI value is adopted in the same frame duration. Therefore, more accurate channel prediction values do not necessarily lead to better CQI prediction values. Normally, stronger correlation can lead to better CQI mapping performance.

**B. SYSTEM MODEL**

In the AMC procedure, the receiver evaluates the channel condition and select suitable modulation index and encoding rate for the next scheduled signal, as shown in Fig. 2. SNR vector or single SNR value can be calculated by the estimated channel parameter, which depends on the channel time-varying level. The estimated SNR is a vector for time-varying channel, which leads to the requirement of calculating effective SNR with SNR mapping algorithm. The effective SNR is utilized to calculate the feedback CQI parameter.

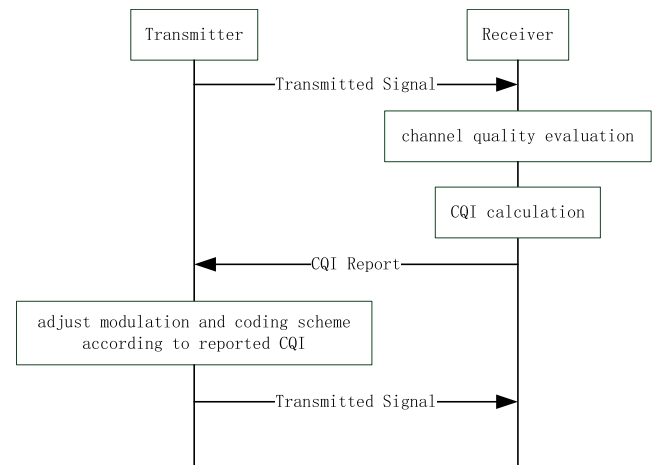


**FIGURE 2. AMC procedure.**

The AMC system model and corresponding parameters of this paper are consistent with the 3GPP long term evolution (LTE) standard [17] and the research results can be adopted not only in LTE system but also in other system with AMC. In LTE specification, Turbo coding and three kinds of modulation methods (QPSK, 16QAM and 64QAM) are adopted. Single UE is usually allocated with multiple physical resource blocks (PRB), which causes the argument that whether adopts consistent MCS in all PRBs occupied by the UE. It was found that the performance of AMC with same CQI is slightly worse than that with different CQIs (different subcarrier adopts different MCS). However, the signal overhead of AMC with same CQI scheme is significantly reduced

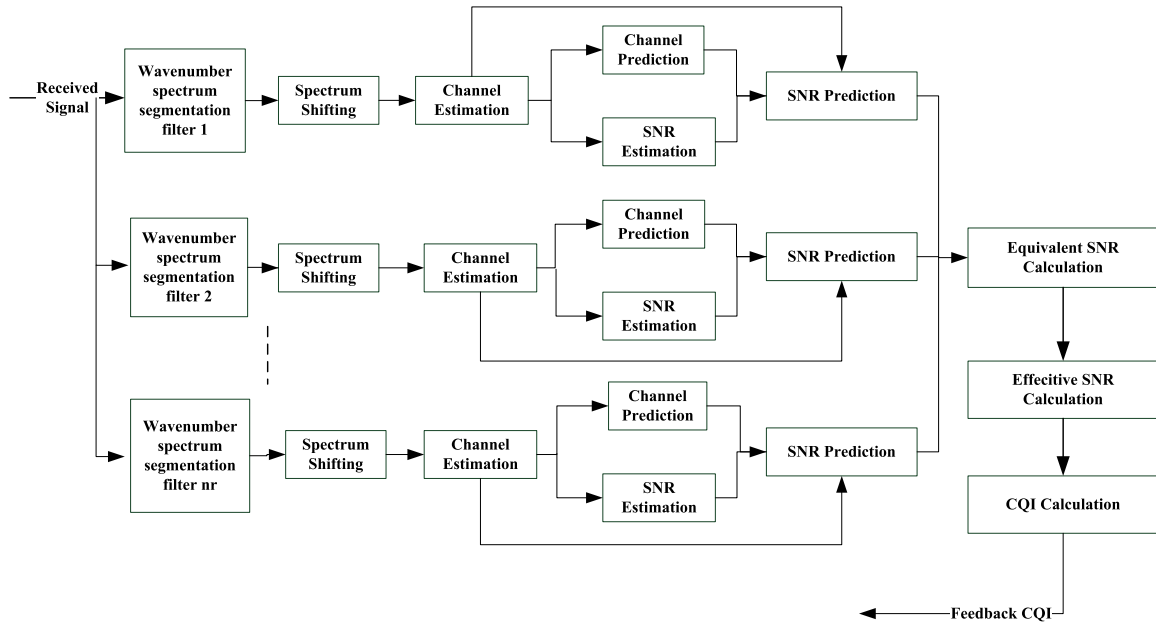


FIGURE 3. Wavenumber spectrum segmentation filters bank based CQI prediction scheme.

compared with the different CQI scheme. Therefore, in this paper, UE is assumed to adopt same MCS in all PRBs at one transmission time interval (TTI).

This paper focuses on the channel quality evaluation of AMC. And the proposed CQI prediction scheme is illustrated in Fig. 3, where multiple antennas with wavenumber spectrum segmentation filters bank is utilized in the receiver side. The channel estimation, channel prediction and signal to noise (SNR) rate prediction are all based on the orthogonal subspace level. Then, the equivalent SNR after subspace combination is calculated according to the combination scheme and effective SNR is obtained through SNR mapping algorithm to calculate the feedback channel quality index (CQI) parameter. And the received baseband sample signal by antenna array after the time-varying multipath channel can be expressed as

$$\mathbf{y}(n) = \sum_{l=1}^L \sum_{p=1}^{N_l} \mathbf{a}(\theta_p^l) h_p^l(n) s(n - \lceil \tau_l / T_s \rceil) \exp(j2\pi f_{\Delta} n T_s) + \boldsymbol{\eta}(n) \quad (1)$$

where  $s(n)$  is the transmit signal,  $L$  is the number of resolvable multipath,  $T_s$  is the sample period,  $f_{\Delta}$  is the frequency offset aroused by the difference of oscillator frequency between transmitter and receiver,  $N_l$  is the number of irresolvable sub-path of the  $l$ -th resolvable multipath,  $\tau_l$  is the time delay of the  $l$ -th resolvable multipath,  $h_p^l(n)$  is the channel parameter at  $nT_s$  of the  $p$ -th irresolvable sub-path in the  $l$ -th resolvable multipath on reference antenna port 1,  $\boldsymbol{\eta}(n)$  represents the noise and interference,  $\theta_p^l$  is the Angle of Arrival (AOA) of the  $p$ -th irresolvable sub-path in the  $l$ -th resolvable multipath,  $n_r$  is the number of antennas in receiver,

$\mathbf{a}(\theta_p^l) = [1 \ a_1(\theta_p^l) \ \dots \ a_{n_r}(\theta_p^l)]^T$ .  $a_i(\theta_p^l)$  is a complex value representing the channel gain relative to reference antenna port 1. As for uniform linear array

$$\mathbf{a}(\theta_p^l) = \begin{bmatrix} 1 & e^{j2\pi f d \sin \theta_p^l / c} & \dots & e^{j2\pi f (n_r - 1) d \sin \theta_p^l / c} \end{bmatrix}^T \quad (2)$$

where  $f, c, d$  is the carrier frequency, speed of light and antenna distance respectively.

In high-speed mobile environment, the Doppler shift of each wireless path is different because of the different AOA in each path. Considering the  $h_p^l(n)$  in (1), the channel parameter can be expressed as

$$h_p^l(n) = \mu_p^l \Gamma_p^l(n) e^{j \frac{2\pi}{\lambda} v n T_s \cos(\theta_p^l - \theta_R)} \quad (3)$$

where  $\mu_p^l$  is the path loss of the  $p$ -th irresolvable sub-path in the  $l$ -th resolvable multipath.  $\theta_R$  is the angle of movement direction, which is defined with respect to the antenna array broadside.  $\lambda$  is the wavelength of carrier,  $v$  is the movement speed.  $\Gamma_p^l(n)$  is the fading complex coefficient at  $nT_s$  of the  $p$ -th irresolvable sub-path in the  $l$ -th resolvable multipath, which can be assumed to be fixed approximately in demodulation symbol period.

### III. CHANNEL QUALITY INDICATOR PREDICTION SCHEME

In high speed mobility environments, due to the fast time-varying fading channel, the performance of conventional AMC cannot meet the system requirements in such a hostile environment mainly because of the CQI mismatch mentioned above. In this section, a wavenumber spectrum segmentation filters bank based AMC scheme in high mobility environment is proposed. The main idea of the proposed scheme is

based on orthogonal subspace projection to suppress the time-varying level of wireless channel with wavenumber spectrum segmentation filters bank, which is described as follows in detail.

**A. WAVENUMBER SPECTRUM SEGMENTATION FILTERS BANK**

In general, the channel time-varying is due to the relative movement of both sides. Normally the base station is stationary, and then the channel time-varying characteristic is actually a manifestation of the receiver position change. And the wireless channel shows the spatially selective property. As a receiver moves through space with constant velocity, the fading may be treated as a function of time instead of space by relating the position  $r$  and the time  $t$  by a simple equation of motion:

$$r = r_0 + vt \tag{4}$$

where  $r_0$  is the position at time  $t = 0$  and often set to zero for simplicity.

The wireless channel is a function of time, frequency, and position. It can be expressed as  $\tilde{h}(t, f, r)$ . And there exists Fourier transform pair:

$$\tilde{h}(t, f, r) \leftrightarrow \tilde{H}(\omega, \tau, w) \tag{5}$$

where  $\omega, \tau, w$  denotes Doppler, delay and wavenumber respectively. The wavenumber is a property of the wave, and is defined as the number of wavelengths per  $2\pi$  length. The angular frequency is the angular change per the unit time, and the wavenumber is the angle change per the unit length, so the wavenumber is the spatial angular frequency. The spatial fading rate variance  $\sigma_r^2$  can be adopted to describe the channel time-varying level aroused from the movement of receiver [18], which can be expressed as

$$\sigma_r^2 = E \left\{ \left| \frac{d [\tilde{h}(r) \exp(-j\bar{w}r)]}{dr} \right|^2 \right\} \tag{6}$$

where the  $r$  represents the displacement along some fixed direction in the space,  $\tilde{h}(r)$  is the wireless channel coefficients.  $\bar{w}$  is the center of wavenumber spectrum and can be expressed as

$$\bar{w} = E [w] = \frac{\int_{-\infty}^{+\infty} wS(w)dw}{\int_{-\infty}^{+\infty} S(w)dw} \tag{7}$$

where  $w$  denotes wavenumber and  $S(w)$  represents the wavenumber spectrum.

Then,

$$\sigma_r^2 = E \{G(r)\} \sigma_w^2 \tag{8}$$

where  $E \{G(r)\}$  is the signal power.  $\sigma_w^2$  is the root mean square (RMS) wavenumber spread which can be expressed as

$$\sigma_w^2 = \frac{\int_{-\infty}^{+\infty} (w - \bar{w})^2 S(w)dw}{\int_{-\infty}^{+\infty} S(w)dw} \tag{9}$$

Therefore, the root mean square wavenumber spread  $\sigma_w^2$  can be adopted to describe the time-varying degree of the equivalent channel in the high-speed mobile environments. Then, the time-varying degree can be suppressed by reducing the wavenumber spread. The wavenumber is essentially the angular frequency of the space, and the receiver adopts the multi-antenna technology. The receive signal can pass through the wavenumber vector spectrum orthogonal segmentation filters bank to reduce the root mean square wavenumber spread on each orthogonal subspace. As shown in Fig. 4, this process is achieved by orthogonal segmentation filtering to cut the wave vector spectrum apart.

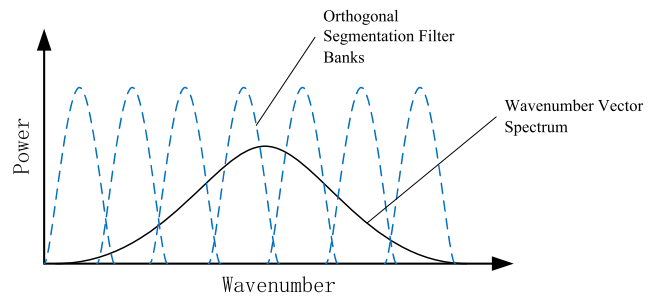


**FIGURE 4. Wavenumber vector spectrum orthogonal segmentation filters bank.**

Define the wavenumber spectrum segmentation filters matrix  $\mathbf{U}_r^T$  as (10)

$$\mathbf{U}_r = [\mathbf{b}^0 \quad \mathbf{b}^1 \quad \dots \quad \mathbf{b}^{n_r-1}] \tag{10}$$

where  $\mathbf{b}^k = [b_0^k \ b_1^k \ \dots \ b_{n_r-1}^k]^T$ ,  $b_q^k$  is the  $q$ -th spatial filter parameter of the  $k$ -th subspace. Actually, the wave number spectrum segmentation filter design is related to the parameter  $b_q^k$ . This parameter can be optimized according to several criteria, such as RMS wavenumber spread minimization criterion

$$\begin{aligned} & [\mathbf{b}^0 \quad \mathbf{b}^1 \quad \dots \quad \mathbf{b}^{n_r-1}]^{opt} \\ &= \arg \min_{[\mathbf{b}^0 \ \mathbf{b}^1 \ \dots \ \mathbf{b}^{n_r-1}]} \left\{ \sum_{k=1}^{n_r} \alpha_k \sigma_{w,k}^2 \right\} \end{aligned} \tag{11}$$

where  $\sigma_{w,k}^2$  is the RMS wavenumber spread in the  $k$ -th subspace and  $\alpha_k$  is the main lobe width of the  $k$ -th wavenumber domain segmentation filter.

Generally, all the spatial domain signal processing methods adopt different weight coefficients value/vector/matrix on different antenna's received signal. Essentially, the beam forming approach in [16] and our wavenumber spectrum segmentation filter bank are both kind of spatial domain signal processing method. The difference between these two approaches lies in the following aspects:

1) Different purposes. Beam forming approach is generally utilized to enhance SNR of received signal and suppress intra-cell/inter-cell interference. Our wavenumber spectrum segmentation filter bank is used to suppress signal time-varying level.

2) Different signal processing methods. Generally, for the same T-R link, each antenna only has only one weighting coefficient in beam forming approach. In the wavenumber spectrum segmentation filter bank approach, each antenna has  $n_r$  weighting coefficients.

3) Different weighting coefficients calculation methods. Generally, the beam forming approach should calculate the weighting coefficients dynamically according to the current channel environments. But the weighting coefficients of the wavenumber spectrum segmentation filter bank approach are not related to the current propagation condition and can be calculated off-line.

4) Different optimization criteria. The weighting coefficients of beam forming approach are generally obtained by SINR maximization or interference power minimization criteria. For the wavenumber spectrum segmentation filter bank approach, RMS wavenumber spread minimization criteria can be utilized.

In brief, the concept of “wavenumber spectrum segmentation filter bank” is actually a kind of spatial domain signal processing method. And we used the concept of “wavenumber spectrum segmentation” is because that we adopt the RMS wavenumber spread to evaluate the wireless channel time-varying level.

The received signal projected into the orthogonal subspaces can be written as

$$\mathbf{y}^a(n) = \mathbf{U}_r^T \mathbf{y}(n) \quad (12)$$

where  $\mathbf{y}^a(n)$  is the signal after wavenumber domain segmentation filters. The  $\mathbf{y}^a(n) = [y_0^a(n) y_1^a(n) \cdots y_{n_r-1}^a(n)]^T$  is a vector with length of  $n_r$ , which is used to evaluate the signal quality for AMC procedure. Moreover, the wavenumber domain segmentation filtered signal in each orthogonal subspace  $y_k^a(n)$  is utilized to estimate the equivalent channel parameter on each orthogonal subspace level. The channel estimation algorithm maybe based on either pilot sequence scheme or blind scheme.

### B. SYMBOL DETECTION FOR TIME-VARIANT CHANNEL

The minimum mean squared error (MMSE) detector is adopted at receiver side. The decoding process can be simplified as

$$\mathbf{z} = \mathbf{H}^H (\mathbf{H}\mathbf{H}^H + \sigma_n^2 \mathbf{I}_N)^{-1} \mathbf{d} \quad (13)$$

where  $\mathbf{z}$  is the estimation vector of transmitted symbol,  $\sigma_n^2$  is the noise power,  $\mathbf{I}_N$  is the  $N - by - N$  identity matrix and  $N$

is the FFT size. The channel matrix  $\mathbf{H}$  is given by (14), as shown at the bottom of this page.

where  $H_k(n) = \sum_{l=0}^{L-1} h_l(n) e^{-j2\pi lk/N}$ ,  $h_l(n)$  is the channel parameter of the  $l$ -th resolvable multipath which can be configured by channel estimation algorithm like basis expansion model (BEM) algorithm [19].

### C. SNR PREDICTION SCHEME

For SNR estimation and prediction, the channel parameters is required. There are many channel estimation methods as BEM algorithm etc. In the proposed SNR prediction scheme, time-variant channel estimation is implemented on each orthogonal after the spectrum shifting process. The shifted channel parameters can be written as

$$\mathbf{H}_{eq}(n) = \mathbf{W} \odot \mathbf{U}_r^T \mathbf{A} \mathbf{H}'(n). \quad (15)$$

where  $\odot$  is Hadamard product,

$$\begin{aligned} \mathbf{A} &= [\mathbf{a}(\theta^0) \quad \mathbf{a}(\theta^1) \quad \cdots \quad \mathbf{a}(\theta^{L-1})], \\ \mathbf{W} &= [\mathbf{w}_1 \quad \mathbf{w}_2 \quad \cdots \quad \mathbf{w}_{n_r}]^T, \\ \mathbf{w}_k &= [e^{-j\bar{w}_k v T_s} \quad e^{-j2\bar{w}_k v T_s} \quad \cdots \quad e^{-j\bar{w}_k v N T_s}]^T, \end{aligned}$$

$\bar{w}_k$  is the center of wavenumber spectrum for the  $k$ -th subspace signal. And channel parameter matrix  $\mathbf{H}'(n)$  can be written as

$$\mathbf{H}'(n) = \begin{bmatrix} h_0(n) & h_0(n+1) & \cdots & h_0(n+N-1) \\ h_1(n) & h_1(n+1) & \cdots & h_1(n+N-1) \\ \vdots & \vdots & \vdots & \vdots \\ h_{L-1}(n) & h_{L-1}(n+1) & \cdots & h_{L-1}(n+N-1) \end{bmatrix}. \quad (16)$$

Then the channel prediction algorithm is utilized to predict the channel parameter in the following frame to compensate the CQI feedback delay. Many channel prediction algorithms can be adopted in this scheme, such as AR and linear extrapolation etc. Moreover, the SNR of current received frame in each orthogonal subspace can also be estimated through estimated channel parameters in each orthogonal subspace.

After obtaining the predicted channel parameter, the predicted SNR in each orthogonal subspace can be calculated as following

$$\gamma_{i,k}^p(n) = \frac{\tilde{h}_{i,k}^2(n)}{\sum_{m=0}^{N-1} h_{i,k}^2(m_0 + m)} \sum_{m=0}^{N-1} \gamma_{i,k}(m_0 + m) \quad (17)$$

$$\mathbf{H} = \frac{1}{\sqrt{N}} \begin{bmatrix} H_0(0) & H_1(0) & \cdots & H_{N-1}(0) \\ H_0(1) & H_1(1) e^{j2\pi/N} & \cdots & H_{N-1}(1) e^{j2\pi(N-1)/N} \\ \vdots & \vdots & \cdots & \vdots \\ H_0(N-1) & H_1(N-1) e^{j2\pi(N-1)/N} & \cdots & H_{N-1}(N-1) e^{j2\pi(N-1)(N-1)/N} \end{bmatrix} \quad (14)$$



where  $\tilde{h}_{i,k}(n)$  represents the predicted channel parameter of the  $i$ -th resolvable multipath in the  $k$ -th orthogonal subspace on the  $n$ -th sampling time, and  $h_{i,k}(n)$  represents the equivalent channel parameter of the  $i$ -th resolvable multipath in the  $k$ -th orthogonal subspace on the  $n$ -th sampling time after wavenumber spectrum shifting,  $m_0$  is the initial sampling time of the frame used to estimate the SNR,  $\gamma_{i,k}^p(n)$  and  $\gamma_{i,k}(n)$  represent the predicted SNR and estimated SNR for the  $i$ -th resolvable multipath in the  $k$ -th orthogonal subspace on the  $n$ -th sampling time respectively.

Finally, the predicted SNR after subspace signal combination should be calculated to evaluate the channel quality. The calculation method is closely related to the signal combination scheme adopted by the receiver. The common combination schemes include maximum ratio combination scheme, equal gain combination scheme and selective combination scheme. Assume that the noise power in each orthogonal subspace is equal. Taking the maximum ratio combination scheme as an example, the predicted SNR after subspace signal combination can be calculated as

$$\gamma^p(n) = \sum_{k=1}^{n_r} \sum_{i=1}^L \gamma_{i,k}^p(n). \quad (18)$$

The predicted SNR vector  $\gamma^p$  with length of  $N$  is utilized to calculate the effective signal to noise ratio  $\gamma_{eff,dB}$ , which will be studied in the following section. Then the  $\gamma_{eff,dB}$  is adopted to look up the SNR threshold table with length 15 corresponding to the number of CQIs defined in the standard. Each of the SNR thresholds is obtained by simulation, which is the SNR corresponding to the BLER equals to 10% with certain CQI in AWGN channel. The proposed CQI prediction scheme procedure can be shown in Fig.2.

In conclusion, the reason that wavenumber spectrum segmentation filters bank can be utilized to improve the performance of AMC scheme lies in that the time-varying level of equivalent wireless channel after wavenumber spectrum segmentation filters on each orthogonal subspace is suppressed and the channel prediction is proceeded also on each orthogonal subspace level. The detailed theoretical analysis will be presented in the following part.

#### D. CQI EVALUATION PROCEDURE

In this section, a scale factor optimization method in effective SNR mapping algorithm is proposed to evaluate the effective SNR. The main reason to calculate the effective SNR is that the instant SNR on each symbol in one frame duration is not a constant because of time-varying channel in high mobility. That means the measured SNR on the frame level is a vector rather than a scalar quantity. However, the reported CQI value is evaluated by looking up the performance table obtained through simulation with corresponding SNR scalar value. Therefore, the measured SNR vector should be mapped to a scalar quantity, which is named as effective SNR.

The evaluation procedure of CQI from received SNR can be simplified as following steps:

- 1) Measure the SNR vector of received signal in one frame duration;
- 2) Map the measured SNR vector to effective SNR;
- 3) Look up the performance table to obtain BLERs in different CQI conditions according to the effective SNR;
- 4) Choose the CQI with corresponding BLER mostly close to 10% as the reporting CQI value.

The ESM algorithm can be summarized as

$$BLER(\boldsymbol{\gamma}) \approx BLER_{AWGN}(\gamma_{eff}) \quad (19)$$

where  $\boldsymbol{\gamma} = [\gamma_1, \gamma_2, \gamma_3, \dots, \gamma_N]$  are SNR vector with length of  $N$ ,  $BLER(\boldsymbol{\gamma})$  represents the actual BLER in the real channel instant corresponding to  $\boldsymbol{\gamma}$ ,  $BLER_{AWGN}(\gamma_{eff})$  is the block error rate in AWGN channel corresponding to  $\gamma_{eff}$ ,  $BLER_{AWGN}$  can be evaluated through computer simulation with different CQIs in advance.

The often used ESM algorithm include the exponential effective SNR mapping (EESM) algorithm and the mutual information effective SNR mapping (MI-ESM) algorithm. The mapping function of EESM algorithm can be expressed as [20]

$$\gamma_{eff} = EESM(\boldsymbol{\gamma}, \beta) = -\beta \ln \left[ \frac{1}{N} \sum_{i=1}^N \exp\left(\frac{\gamma_i}{\beta}\right) \right] \quad (20)$$

where  $\beta = \gamma_{mod} \gamma_{cod} \cdot \beta$  is the scale factor determined by modulation and coding scheme.  $\gamma_{mod}$  is the adjusting factor for modulation method, and  $\gamma_{cod}$  is the adjusting factor for coding rate.

The effective SNR mapping procedure of MI-ESM algorithm is defined as [21]

$$\gamma_{eff} = \beta I^{-1} \left[ \frac{1}{N} \sum_{i=1}^N I_m \left( \frac{\gamma_i}{\beta} \right) \right] \quad (21)$$

where  $I_m(x)$  is the compression function, which represents the channel mutual information function with modulation index  $m$ . The mutual information function  $I_m(x)$  represents the amount of information per symbol at certain SNR condition.

It is needed to emphasize that our proposed scheme utilizes the predicted SNR vector  $\boldsymbol{\gamma}^p$  rather than the original time-varying SNR vector to calculate the one CQI value for the whole frame. This makes the CQI mapping more accurate because the correlation of the wireless channel in each orthogonal subspace is enhanced by the wavenumber spectrum segmentation filters and spectrum shifting. That means the degree of time variation of the predicted SNR vector  $\boldsymbol{\gamma}^p$  is relatively lower than that of the original time-varying SNR vector. Fig. 5 shows the throughput performance for different channel variation level. The ‘‘slow channel variation’’ refers to the throughput of AMC system adopting linear variation channel model with a slope of 0.5, and the ‘‘fast channel variation’’ represents a slope of 0.8. Ideal channel prediction is adopted in the receiver. It shows that the throughput performance of AMC with slow variation channel is better than that with fast variation channel. This can be ascribed to the

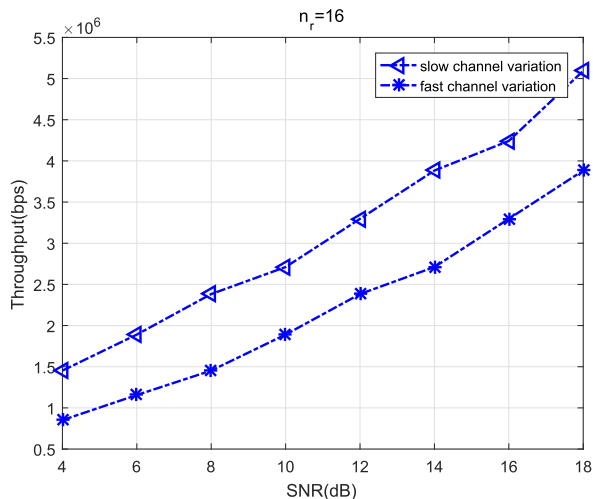


FIGURE 5. AMC throughput performance under different channel time-varying level.

fact that the less CQI mapping mismatch is achieved with the stronger correlation channel.

#### IV. PERFORMANCE ANALYSIS AND SIMULATIONS

In this section, autocorrelation function and spatial fading rate variance for our proposed scheme are derived respectively. Then, the throughput performance of proposed scheme is compared with that of [16] and [22] with simulation results.

##### A. AUTOCORRELATION WITH $n_r$

The conventional power spectrum  $P(f)$  of the received signal can be expressed as

$$P(f) = \frac{P_{av}}{2\pi f_{max}^d \sqrt{1 - \left(\frac{f-f_c}{f_{max}^d}\right)^2}} \quad |f - f_c| \leq f_{max}^d \quad (22)$$

where the  $f_{max}^d$  is the equivalent maximum Doppler shift,  $P_{av}$  is the average power of received signal and  $f_c$  is the carrier of received signal.

The power spectrum  $P_k(f)$  of received signal in the  $k$ -th orthogonal subspace after wavenumber spectrum segmentation filters bank can be expressed as

$$P_k(f) = \frac{P_{av}}{2\pi f_{max}^d \sqrt{1 - \left(\frac{f-f_c}{f_{max}^d}\right)^2}} \quad f_{min}^k \leq f - f_c \leq f_{max}^k. \quad (23)$$

The power spectrum  $P_k(f + f_{min}^k)$  of received signal in the  $k$ -th orthogonal subspace after spectrum shifting can be expressed as

$$\begin{aligned} &P_k(f + f_{min}^k) \\ &= \frac{P_{av}}{2\pi f_{max}^d \sqrt{1 - \left(\frac{f+f_{min}^k-f_c}{f_{max}^d}\right)^2}} \quad 0 \leq f - f_c \leq f_{max}^k - f_{min}^k \end{aligned} \quad (24)$$

where  $f_{min}^k$  is the minimum Doppler frequency of the  $k$ -th orthogonal subspace and  $f_{max}^k$  is the maximum Doppler frequency of the  $k$ -th orthogonal subspace.

To simplify this discussion, we analyze the power spectrum of received signal including the  $k$ -th and the  $(n_r - k)$ -th orthogonal subspace, then define

$$P'_k(f) \triangleq \begin{cases} \frac{P_{av}}{2\pi f_{max}^d \sqrt{1 - \left(\frac{f+f_{min}^k-f_c}{f_{max}^d}\right)^2}} & 0 \leq f - f_c \leq f_{max}^k - f_{min}^k \\ \frac{P_{av}}{2\pi f_{max}^d \sqrt{1 - \left(\frac{f-f_{min}^k-f_c}{f_{max}^d}\right)^2}} & -f_{max}^k + f_{min}^k \leq f - f_c \leq 0. \end{cases} \quad (25)$$

The inverse Fourier transform of (25) is

$$\begin{aligned} R_k(\tau) &= \int_{-\infty}^{\infty} P'_k(f) e^{j2\pi f \tau} df \\ &= \frac{P_{av}}{\pi f_{max}^d} \int_0^{f_{max}^k - f_{min}^k} \frac{\cos 2\pi f \tau}{\sqrt{1 - \left(\frac{f+f_{min}^k-f_c}{f_{max}^d}\right)^2}} df. \end{aligned} \quad (26)$$

So the autocorrelation of received signal after subspace combination is

$$\begin{aligned} R(\tau) &= \sum_{k=1}^{n_r} R_k(\tau) \\ &= \sum_{k=1}^{n_r} \frac{P_{av}}{\pi f_{max}^d} \int_0^{f_{max}^k - f_{min}^k} \frac{\cos 2\pi f \tau}{\sqrt{1 - \left(\frac{f+f_{min}^k-f_c}{f_{max}^d}\right)^2}} df. \end{aligned} \quad (27)$$

Fig. 6 is presented under the assumption that the wavenumber spectrum segmentation filters divide the subspaces with equal width in wavenumber domain. As shown in Fig.6, the autocorrelation of channel is related to the order of wavenumber spectrum segmentation filters  $n_r$ . With the  $n_r$  increasing, the performance of the autocorrelation of channel improve significantly, which confirms that the correlation of the wireless channel in each orthogonal subspace is enhanced by the wavenumber spectrum segmentation filters. Therefore, the channel time-varying level can be suppressed through increasing the number of antennas in receiver. Furthermore, the autocorrelation curve of  $n_r = 16$  tends to be small at the time delay  $\tau = 4NT_s$ , which means that the correlation of channel parameters is weaker at this time interval. Fig. 7 compares the correlation of channel parameters between spectrum shifting and none spectrum shifting. It shows that the channel parameters correlation of the orthogonal subspace with wavenumber spectrum shifting is much better than that without wavenumber spectrum shifting.

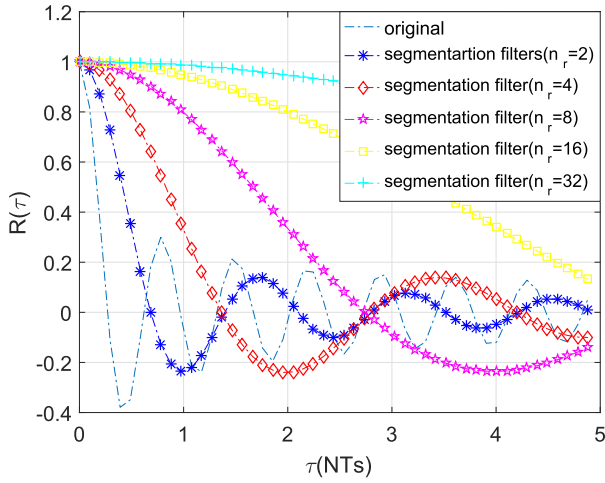


FIGURE 6. Normalized autocorrelation of proposed scheme and conventional scheme ( $v=300$  km/h,  $N=1024$ ).

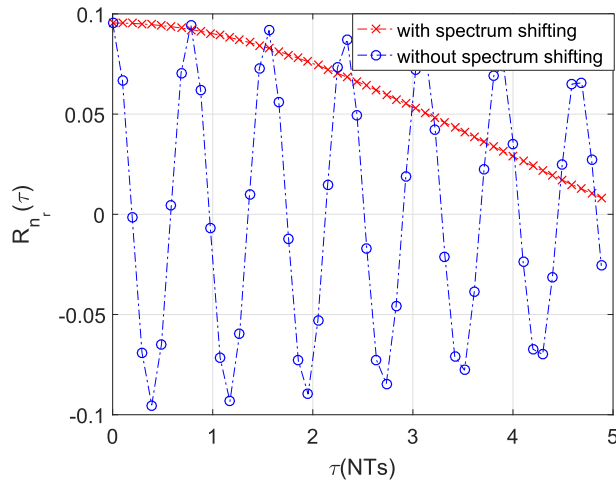


FIGURE 7. Autocorrelation comparison of the  $n_r$ -th orthogonal subspace between with spectrum shifting and without spectrum shifting ( $v=300$  km/h,  $n_r = 16$ ,  $N=1024$ ).

**B.  $\sigma^2$  WITH  $n_r$**

In this part, the principle of proposed wavenumber vector spectrum orthogonal segmentation filters bank method to improve the performance of AMC is presented. As mentioned above, the main reason resulting in the performance deterioration of general AMC scheme in high mobility situation is the weakened correlation of wireless channel parameters, which is caused by the time-varying characteristic. Essentially, solutions to the problem should suppress the time-varying level of wireless channel parameters. Assuming the AOA is uniform distributed around the receiver antennas and no angle resolution ambiguity is assumed. The azimuth spectrum in  $k$ -th subspace can be expressed as

$$\rho_k(\theta) = \begin{cases} \frac{1}{\alpha_k} & \frac{\pi}{2} - \theta_k - \frac{\alpha_k}{2} \leq \theta \leq \frac{\pi}{2} - \theta_k + \frac{\alpha_k}{2} \\ 0 & \text{Others} \end{cases} \quad (28)$$

where the  $\alpha_k$  ( $0 \leq \alpha_k \leq \pi$ ) is the width of sector in  $k$ -th subspace and  $\theta_k$  is the angle offset of  $k$ -th subspace with  $(0 \leq \theta_k - \frac{\alpha_k}{2} \leq \theta_k + \frac{\alpha_k}{2} \leq \pi)$ .

The relationship between wavenumber spectrum and azimuth spectrum can be expressed as

$$S_k(w) = \rho_k(\theta) \left| \frac{d\theta}{dw} \right| \quad (29)$$

Then the  $\bar{w}_k$  can be calculated as

$$\begin{aligned} \bar{w}_k &= E[w_k] \\ &= \frac{\int_{-\infty}^{+\infty} w S_k(w) dw}{\int_{-\infty}^{+\infty} S_k(w) dw} \\ &= \frac{w_0}{\alpha_k} \left[ \sin\left(\theta_k + \frac{\alpha_k}{2}\right) - \sin\left(\theta_k - \frac{\alpha_k}{2}\right) \right] \\ &= \frac{2w_0}{\alpha} \cos \theta_k \sin \frac{\alpha_k}{2} \end{aligned} \quad (30)$$

where  $w_0 = 2\pi/\lambda$ . Then the root mean square wavenumber spread in  $k$ -th subspace  $\sigma_{w,k}^2$  can be calculated as

$$\begin{aligned} \sigma_{w,k}^2 &= \frac{\int_{-\infty}^{+\infty} (w - \bar{w}_k)^2 S_k(w) dw}{\int_{-\infty}^{+\infty} S_k(w) dw} \\ &= \frac{w_0^2}{2} \left( 1 - \sin^2\left(\frac{\alpha_k}{2\pi}\right) \right) \\ &\quad \times \left( 1 - \frac{\sin^2\left(\frac{\alpha_k}{2\pi}\right) - \sin^2\left(\frac{\alpha_k}{\pi}\right) \cos(2\theta_k)}{1 - \sin^2\left(\frac{\alpha_k}{2\pi}\right)} \right) \end{aligned} \quad (31)$$

Then,

$$\begin{aligned} \frac{d\sigma_{w,k}^2}{d\alpha_k} &= w_0^2 \left( -\frac{\sin\alpha_k}{2\alpha_k^2} (2 + 3 \cos 2\theta_k) + \frac{1}{2\alpha_k} (\cos(\alpha_k) \cos(2\theta_k)) \right. \\ &\quad \left. + \frac{2}{\alpha_k^3} ((1 + \cos 2\theta_k) (1 - \cos \alpha_k)) \right) \end{aligned} \quad (32)$$

Numerical analysis shows that the  $\frac{d\sigma_{w,k}^2}{d\alpha_k}$  reach the maximum when  $\theta_k = 0$  and  $\theta_k = \pi$ . Then

$$\begin{aligned} \max_{0 \leq \theta_k \leq \pi} \left\{ \frac{d\sigma_{w,k}^2}{d\alpha_k} \right\} &= w_0^2 \left( -\frac{5\sin\alpha_k}{2\alpha_k^2} + \frac{1}{2\alpha_k} \cos(\alpha_k) \right. \\ &\quad \left. + \frac{4}{\alpha_k^3} (1 - \cos \alpha_k) \right) \end{aligned} \quad (33)$$

To simplify the analysis, the wavenumber vector spectrum orthogonal segmentation filters bank is assumed to divide the received signal in wavenumber domain with equal  $\alpha_k$ , which means that  $\alpha_k = \frac{\pi}{n_r}$ . Then the  $d\sigma_{w,k}^2/dn_r$  can be expressed as

$$\begin{aligned} \max_{0 \leq \theta_k \leq \pi} \left\{ \frac{d\sigma_{w,k}^2}{dn_r} \right\} &= \max_{0 \leq \theta_k \leq \pi} \left\{ \frac{d\sigma_{w,k}^2}{d\alpha_k} \right\} \frac{d\alpha_k}{dn_r} \\ &= w_0^2 \left( \frac{5\sin\frac{\pi}{n_r}}{2\pi} - \frac{1}{2n_r} \cos\left(\frac{\pi}{n_r}\right) - \frac{4n_r}{\pi^2} \left( 1 - \cos\frac{\pi}{n_r} \right) \right) \end{aligned} \quad (34)$$



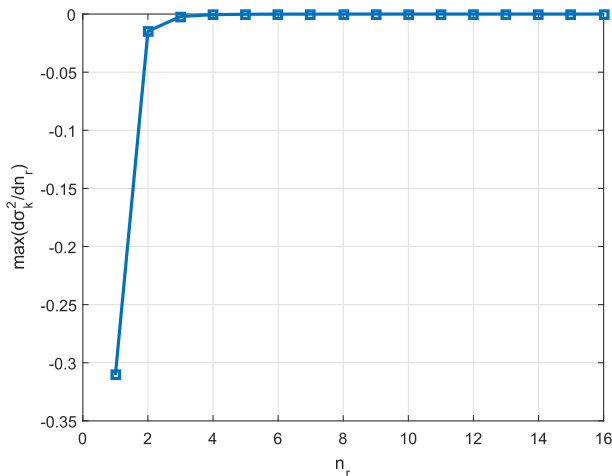


FIGURE 8.  $d\sigma_{w,k}^2/(dn_r w_0^2)$  with  $n_r$ .

The Fig. 8 shows the  $\max_{0 \leq \theta_k \leq \pi} \left\{ \frac{d\sigma_{w,k}^2}{dn_r} \right\}$  with  $n_r$ . We find that the equation  $\max_{0 \leq \theta_k \leq \pi} \left\{ \frac{d\sigma_{w,k}^2}{dn_r} \right\} = 0$  has no positive real number solution through numerical calculation and the limit of  $\max_{0 \leq \theta_k \leq \pi} \left\{ \frac{d\sigma_{w,k}^2}{dn_r} \right\}$  when the number of antennas  $n_r$  approaches to the positive infinity is

$$\begin{aligned} & \lim_{n_r \rightarrow \infty} \max_{0 \leq \theta_k \leq \pi} \left\{ \frac{d\sigma_{w,k}^2}{dn_r} \right\} \\ &= \lim_{n_r \rightarrow \infty} \left( w_0^2 \left( \frac{5 \sin \frac{\pi}{n_r}}{2\pi} - \frac{1}{2n_r} \cos \left( \frac{\pi}{n_r} \right) \right. \right. \\ & \quad \left. \left. - \frac{4n_r}{\pi^2} \left( 1 - \cos \frac{\pi}{n_r} \right) \right) \right) \\ &= w_0^2 \lim_{n \rightarrow \infty} \left( -\frac{4n_r}{\pi^2} \left( 1 - \cos \frac{\pi}{n_r} \right) \right) = 0 \quad (35) \end{aligned}$$

Obviously, the  $\max_{0 \leq \theta_k \leq \pi} \left\{ \frac{d\sigma_{w,k}^2}{dn_r} \right\}$  is an elementary complex function of  $n_r$  and is a continuous function. Because the  $\max_{0 \leq \theta_k \leq \pi} \left\{ \frac{d\sigma_{w,k}^2}{dn_r} \right\} \Big|_{n_r=1} < 0$ , we have  $\max_{0 \leq \theta_k \leq \pi} \left\{ \frac{d\sigma_{w,k}^2}{dn_r} \right\} < 0$  and  $d\sigma_{w,k}^2/dn_r < 0$ , which means  $\sigma_{w,k}^2$  becomes smaller when the  $n_r$  becomes larger. Therefore, the channel time-varying level can be suppressed through increasing the number of antennas in receiver. That is to say, we can enhance the correlation of wireless channel in each orthogonal subspace through wavenumber vector spectrum orthogonal segmentation filters bank. Because the proposed scheme predicts the channel parameters and SNR on subspace level, the obtained CQI value can match the channel condition better in high mobility environments.

C. SIMULATIONS AND ANALYSIS

In this section, to verify the ability to support the time-varying channel environment of proposed method, the performance

of proposed wavenumber spectrum segmentation filters bank based AMC scheme is presented and compared. Then the performance of the proposed scale factor optimization method is evaluated.

In the simulation, 5GHz carrier frequency and 300 km/h movement speed are considered. Raleigh fading channel model is adopted, where the number of resolvable multipath  $L=1$ , the number of irresolvable sub-path of  $l$ -th resolvable multipath  $N_l = 400$  and the distribution of sub-paths' AOA is uniform distributed from 0 to  $2\pi$ . The situation of proposed scheme with the number of resolvable multipath  $L \geq 2$  is similar. To evaluate the performance of the proposed scheme, we use the AMC modes defined in the 3GPP long term evolution (LTE) standard (Table 7.2.3-1) [17], as shown in Tab.I. Single carrier system with rate matching and turbo code is adopted in the simulation system model. All the simulation results are obtained based on ideal channel estimation condition, which means that the receiver is assumed to know the accurate wireless channel parameters.

TABLE 1. CQI table.

CQI index	modulation	code rate x 1024	efficiency
0	out of range		
1	QPSK	78	0.1523
2	QPSK	120	0.2344
3	QPSK	193	0.3770
4	QPSK	308	0.6016
5	QPSK	449	0.8770
6	QPSK	602	1.1758
7	16QAM	378	1.4766
8	16QAM	490	1.9141
9	16QAM	616	2.4063
10	64QAM	466	2.7305
11	64QAM	567	3.3223
12	64QAM	666	3.9023
13	64QAM	772	4.5234
14	64QAM	873	5.1152
15	64QAM	948	5.5547

Fig. 9 shows the AMC throughput performance of the different schemes for different CQI feedback delay under Rayleigh fading channel. It shows that the performance of proposed scheme is better than that of other schemes. This can be ascribed to the fact that the performance of channel prediction algorithm falls tremendously because of the little relativity of wireless channel in AMC scheme. The reason of performance gap between proposed scheme and AR-BF scheme [16] mainly lies on that: proposed scheme adopts the wavenumber spectrum shifting to suppress the time-varying level caused by high mobility on each orthogonal subspace, which decrease the mismatch level of CQI mapping. In additional, the computational complexity of AR model  $O(\kappa \zeta^2 - \zeta^3) \approx O(\zeta^3)$  ( $\kappa \geq 2\zeta$ ) adopted by AR-BF is much higher than that of linear extrapolation algorithm  $O(\zeta)$

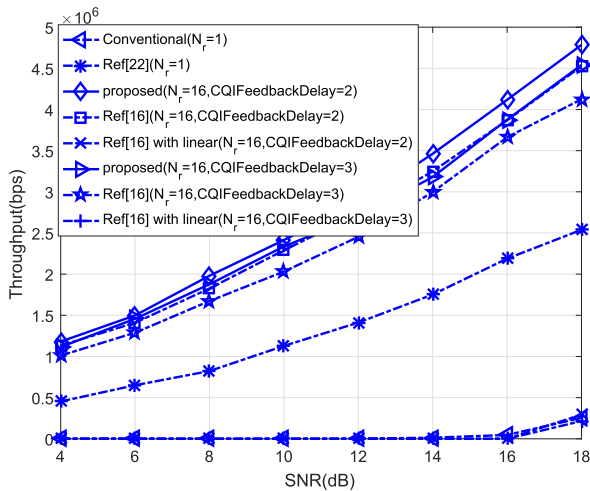


FIGURE 9. AMC throughput performance with multiple frames feedback delay.

adopted by our proposed scheme, where the  $\zeta$  is the order of AR model and  $\kappa$  is the modeling data length. A suitable order of the predictor strongly depends on fading conditions. In most case, a predictor order  $\zeta$  of around 40-50 is reasonable [23]. And we notice that the throughput performance of method in [16] with linear extrapolation algorithm deteriorates severely. On the other hand, compared with traditional AMC scheme or AMC scheme based on dynamically adjusting back-off factor in [22], the improvement of proposed scheme is quite significant. This comes from the fact that the relativity of wireless channel is enhanced by wave number spectrum segmentation filters in proposed scheme. Moreover, the proposed AMC scheme obtain better performance and can predict the channel condition better even for larger CQI feedback delay.

V. CONCLUSION

In high speed mobility scenes, the performance of general AMC technology is strictly limited with the mismatch of CQI under fast time-varying channels. To deal with the problem, a channel quality indicator prediction scheme based on wavenumber spectrum segmentation filters bank in high speed mobility environment is proposed in this paper, which utilizes wavenumber spectrum segmentation filters bank to enhance the equivalent wireless channel parameters correlation in temporal domain and reduce the CQI mapping mismatch level. The theoretical analysis and simulation results show that the proposed channel quality indicator prediction scheme improves the accuracy of CQI prediction with lower complexity in high speed mobility environment.

REFERENCES

[1] IMT-2020(5G) Promotion Group, "5G network technology architecture," IMT-2020, China, White Paper IMT-2020, 2015. [Online]. Available: <http://www.imt-2020.org.cn/en>

[2] J. Hayes, "Adaptive feedback communications," *IEEE Trans. Commun. Technol.*, vol. COM-16, no. 1, pp. 29-34, Feb. 1968.

[3] J. C. Hancock and W. C. Lindsey, "Optimum performance of self-adaptive systems operating through a Rayleigh-fading medium," *IEEE Trans. Commun. Syst.*, vol. 11, no. 4, pp. 443-453, Dec. 1963.

[4] J. K. Cavers, "Variable-rate transmission for Rayleigh fading channels," *IEEE Trans. Commun.*, vol. COMM-20, no. 1, pp. 15-22, Feb. 1972.

[5] J. Meng and E. H. Yang, "Constellation and rate selection in adaptive modulation and coding based on finite blocklength analysis and its application to LTE," *IEEE Trans. Wireless Commun.*, vol. 13, no. 10, pp. 5496-5508, Oct. 2014.

[6] L. Wan et al., "Adaptive modulation and coding for underwater acoustic OFDM," *IEEE J. Ocean. Eng.*, vol. 40, no. 2, pp. 327-336, Apr. 2015.

[7] A. Farrokh, V. Krishnamurthy, and R. Schober, "Optimal adaptive modulation and coding with switching costs," *IEEE Trans. Commun.*, vol. 57, no. 3, pp. 697-706, Mar. 2009.

[8] S.-K. Ahn and K. Yang, "Adaptive modulation and coding schemes based on LDPC codes with irregular modulation," *IEEE Trans. Commun.*, vol. 58, no. 9, pp. 2465-2470, Sep. 2010.

[9] S. Sun, K. Yang, J. Wu, D. Zhu, and M. Lei, "Adaptive modulation and coding for two-way relaying with amplify-and-forward protocols," *IET Commun.*, vol. 8, no. 7, pp. 1017-1023, May 2014.

[10] A. Duel-Hallen, "Fading channel prediction for mobile radio adaptive transmission systems," *Proc. IEEE*, vol. 95, no. 12, pp. 2299-2313, Dec. 2007.

[11] K. E. Baddour and N. C. Beaulieu, "Autoregressive modeling for fading channel simulation," *IEEE Trans. Wireless Commun.*, vol. 4, no. 4, pp. 1650-1662, Jul. 2005.

[12] L. Fan, Q. Wang, Y. Huang, and L. Yang, "Performance analysis of low-complexity channel prediction for uplink massive MIMO," *IET Commun.*, vol. 10, no. 14, pp. 1744-1751, Sep. 2016.

[13] R. Zeng, Y. Yao, and X. Fang, "Multiple antennas angle domain resolution based transceiver algorithm for high-speed mobile environment," *J. Electron. Inf. Technol.*, vol. 34, no. 9, pp. 2218-2223, 2013.

[14] R. Zeng, X. Fang, and Z.-Q. Yi, "Orthogonal angle domain subspace projection based time-frequency synchronization algorithm for high-speed mobile environment," *Tien Tzu Hsueh Pao/Acta Electronica Sinica*, vol. 41, no. 10, pp. 2094-2099, 2013.

[15] R. Zeng, H. Huang, L. Yang, and Z. Zhang, "Joint estimation of frequency offset and Doppler shift in high mobility environments based on orthogonal angle domain subspace projection," *IEEE Trans. Veh. Technol.*, vol. 67, no. 3, pp. 2254-2266, Mar. 2018.

[16] T. Svantesson and A. L. Swindlehurst, "A performance bound for prediction of MIMO channels," *IEEE Trans. Signal Process.*, vol. 54, no. 2, pp. 520-529, Feb. 2006.

[17] *Physical Layer Procedures*, TS 36.213 V15.0.0, 3GPP, 2017.

[18] G. D. Durgin, *Space-Time Wireless Channels*. Upper Saddle River, NJ, USA: Prentice-Hall, 2003.

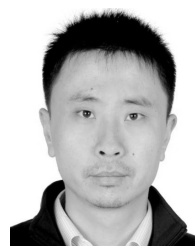
[19] Y.-S. Choi, P. J. Voltz, and F. A. Cassara, "On channel estimation and detection for multicarrier signals in fast and selective Rayleigh fading channels," *IEEE Trans. Commun.*, vol. 49, no. 8, pp. 1375-1387, Aug. 2001.

[20] S. N. Donthi and N. B. Mehta, "An accurate model for EESM and its application to analysis of CQI feedback schemes and scheduling in LTE," *IEEE Trans. Wireless Commun.*, vol. 10, no. 10, pp. 3436-3448, Oct. 2011.

[21] Z. Yermeche, P. Cornelius, N. Grbic, and I. Claesson, "Spatial filter bank design for speech enhancement beamforming applications," in *Proc. Sensor Array Multichannel Signal Process. Workshop*, Jul. 2004, pp. 557-560.

[22] P. Hosein, "Adaptive algorithm for mapping channel quality information to modulation and coding schemes," in *Proc. IEEE 69th Veh. Technol. Conf.*, Apr. 2009, pp. 1-3.

[23] D. Jarinová, "On autoregressive model order for long-range prediction of fast fading wireless channel," *Telecommun. Syst.*, vol. 52, no. 3, pp. 1533-1539, 2013, doi: 10.1007/s11235-011-9520-6.



**RONG ZENG** was born in Jiangsu, China, in 1976. He received the Ph.D. degree in electrical engineering from Southeast University, Nanjing, China, in 2004. From 2004 to 2006, he was a System and Algorithm Engineer with COMMIT Incorporation, Shanghai, China. From 2015 to 2016, he was a Visiting Scholar with the Department of Electrical and Computer Engineering, Colorado State University, Fort Collins, CO, USA. He is currently an Associate Professor with the School of Communication Engineering, Hangzhou Dianzi University, Hangzhou, China. His research interests include 5G wireless systems, the IoT, and V2X.



**TIANJING LIU** was born in Zhejiang, China, in 1993. He received the M.S. degree in communication engineering from Hangzhou Dianzi University, Hangzhou, China, in 2019. His research interests include wireless access technology and V2X.



**XUTAO YU** received the Ph.D. degree from the National Mobile Communication Research Laboratory, Southeast University, Nanjing, China, in 2004, where she is currently a Full Professor with the State Key Laboratory of Millimeter Waves. Her current research interests include quantum computing in wireless networks and quantum communication networks.



**ZAICHEN ZHANG** was born in Nanjing, China, in 1975. He received the B.S. and M.S. degrees in electrical and information engineering from Southeast University, Nanjing, in 1996 and 1999, respectively, and the Ph.D. degree in electrical and electronic engineering from The University of Hong Kong, Hong Kong, in 2002. From 2002 to 2004, he was a Postdoctoral Fellow with the National Mobile Communications Research Laboratory, Southeast University. He joined the School of Information Science and Engineering, Southeast University, in 2004, where he is currently a Professor. He has published over 150 papers and holds issued 20 patents. His current research interests include 5G wireless systems, optical wireless communication technologies, and quantum information transmission.

• • •